# Accounting for Gravitational Attraction and Loading Effects from Land Ice on Absolute Sea Level

RUI M. PONTE, KATHERINE J. QUINN, AND CHRISTOPHER G. PIECUCH

*Atmospheric and Environmental Research, Inc., Lexington, Massachusetts*

(Manuscript received 16 May 2017, in final form 13 December 2017)

ABSTRACT

Gravitational attraction and loading (GAL) effects associated with ongoing long-term changes in land ice are expected to cause spatially varying trends in absolute sea level $\zeta$, as measured by satellite altimeters. The largest spatial gradients in $\zeta$ trends, predicted from solving the sea level equation using GRACE retrievals of mass distribution over land for the period 2005–15, occur near Greenland and West Antarctica, consistent with a strong local land ice loss. Misinterpreting the estimated static GAL trends in $\zeta$ as dynamic pressure gradients can lead to substantial errors in large-scale geostrophic transports across the Southern Ocean and the subpolar North Atlantic over the analyzed decade. South of Greenland, where altimeter sea level and hydrography (Argo) data coverage is good, the residual $\zeta$ minus steric height trends are similar in magnitude and sign to the gravitationally based predictions. In addition, estimated GAL-related trends are as large—if not larger than—other factors, such as deep steric height, dynamic bottom pressure, and glacial isostatic rebound. Thus, accounting for static GAL effects on $\zeta$ records, which are commonly neglected in oceanographic studies, seems important for a quantitative interpretation of the observed $\zeta$ trends.

## 1. Introduction

The redistribution of water, ice, and air over land, even without involving net mass transfers to the ocean, affects the oceanic mass and sea level fields through the physics of gravitational attraction and loading (GAL; Farrell and Clark 1976; Conrad and Hager 1997; Mitrovica et al. 2001). Processes associated with GAL act on a variety of time scales and have been shown to cause measurable seasonal fluctuations in relative sea level, as seen by tide gauges (Tamisiea et al. 2010), and in situ bottom pressure (Vinogradova et al. 2010). Of particular interest are the trends expected to occur from the melting of the ice sheets, which lead to so-called sea level fingerprints (Conrad and Hager 1997; Mitrovica et al. 2001). Detection of these fingerprints, which could shed light and even possibly constrain the behavior of the ice sheets, is made difficult by the presence of background variability and the noisy nature of various datasets (Kopp et al. 2010; Spada and Galassi 2016). Comprehensive spectral analysis of satellite altimetric measurements, after correcting for steric signals using temperature and salinity data, suggests that only for spherical harmonic degree 2 trends are ice changes detectable at the present time (Spada and Galassi 2016), a result also borne out by analyses of polar motion data (Adhikari and Ivins 2016).

More relevant from an oceanographic perspective emphasized here, the determination of GAL effects on absolute sea level $\zeta$ is also important in order to interpret the altimeter records correctly. Gridded altimetric $\zeta$ fields are taken to represent dynamic topography and used in calculations of surface currents (Le Traon and Morrow 2001). Given that GAL-related effects on $\zeta$ are mostly static in nature for the long time scales of interest (Vinogradova et al. 2015), if not corrected in the altimeter records they can lead to wrong inferences about surface pressure gradients and geostrophic currents. In addition, uncorrected GAL effects can corrupt the inference of trends in steric height and related ocean heat content. For the same reason, the effects of atmospheric pressure at low frequencies, which lead to similar static effects on $\zeta$, are routinely corrected for using the inverted barometer approximation (Chelton et al. 2001; Ponte and Vinogradov 2007).

Over the past decade, several observational platforms—satellite altimetry and gravimetry, as well as the Argo float system—have matured to produce high-quality continuous records of $\zeta$, mass redistribution, and in situ temperature and salinity data in the upper

*Corresponding author*: Rui M. Ponte, rponte@aer.com

DOI: 10.1175/JTECH-D-17-0092.1

ocean. Here, we take advantage of these observations to assess the potential errors in interpretation of $\zeta$ records arising from ignored GAL effects of melting ice sheets and other mass redistributions over land. The results indicate that the common practice of neglecting GAL effects on $\zeta$ is not ideal and that implementing a static correction for GAL effects may be a feasible alternative.

## 2. Data and methodology

Our analyses focus on the period 2005–15, for which we have the best coverage from both Argo and satellite gravimetry. For mass redistribution over land at monthly time scales, we use the latest mascon solutions from the Gravity Recovery and Climate Experiment (GRACE) mission produced by the Jet Propulsion Laboratory (Watkins et al. 2015). These fields represent not only changes in the polar ice sheets but also in glaciers and terrestrial water storage in general, as observed by GRACE. Respective GAL effects on $\zeta$, denoted as $\zeta_L$, were calculated via the so-called sea level equation (Farrell and Clark 1976), an integral equation describing gravitationally consistent spatial variations in sea level that arise from mass redistributions on Earth's surface. We use an iterative pseudospectral approach to solve the sea level equation (Mitrovica and Peltier 1991; Kendall et al. 2005), with elastic components only and rotational feedback included (e.g., Tamisiea et al. 2010; Rietbroek et al. 2012; Jensen et al. 2013). Similar determinations of the effects of atmospheric mass over land on $\zeta$, denoted as $\zeta_A$, were calculated based on surface pressure fields from the GRACE background model, which uses meteorological analysis fields from the Integrated Forecast System of the European Centre for Medium-Range Weather Forecasts (Dobslaw et al. 2013; Flechtner et al. 2015).

We estimate the steric sea level from monthly Argo grids of in situ temperature and salinity produced by the Scripps Institution of Oceanography (Roemmich and Gilson 2009). These grids range from 65°S to 65°N and down to ~2000 m, with reduced data coverage in sea ice–covered or shallow regions. Steric heights were derived from temperature and salinity as per Gill and Niiler (1973).

The effects on sea level from steric height changes below 2000 m, as well as from mass changes related to bottom pressure, are also inferred from a recent global ocean state estimate available from the project for Estimating the Circulation and Climate of the Ocean (ECCO). More specifically, we use the ECCO, version 4, release 3, solution described in detail by Fukumori et al. (2017) and Forget et al. (2015), which covers the period 1992–2015.

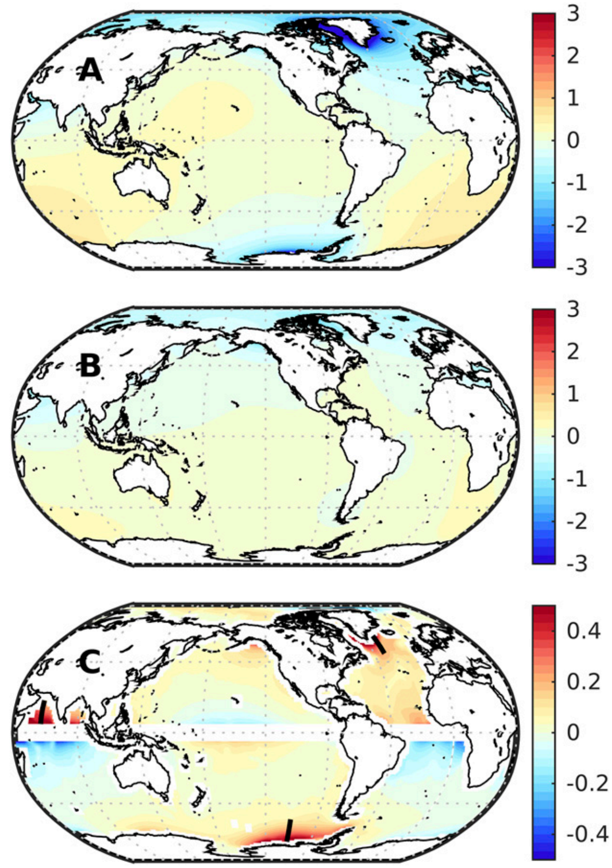


FIG. 1. Trends (mm yr$^{-1}$) in $\zeta$ caused by GAL effects related to changes in (a) land water, including ice sheets and glaciers; and (b) land water, excluding Greenland and Antarctica. Period of analysis is 2005–15, and the time series of the spatial mean field are removed at each grid point prior to trend estimation. (c) Estimated decadal changes in zonal geostrophic transport per degree latitude away from the equator (Sv), based on the GAL trends shown in (a) and assuming they represent a depth-independent pressure gradient. Three sections for which summed transports are quoted in the text are also indicated (thick black lines).

Monthly 1° × 1° gridded altimeter data were obtained from the Commonwealth Scientific and Industrial Research Organisation in Australia (Watson et al. 2015). These data are a combination of TOPEX/Poseidon, *Jason-1*, and *Jason-2*/Ocean Surface Topography Mission (OSTM). In addition to standard corrections (sea state bias, tides, etc.), an inverted barometer and glacial isostatic adjustment correction have been applied.

All time series have been analyzed by doing a joint least squares fit for trend and annual components, and trend results are emphasized in what follows.

## 3. Results

In the absence of GAL effects, and aside from dynamical effects ignored for the purpose of this discussion,

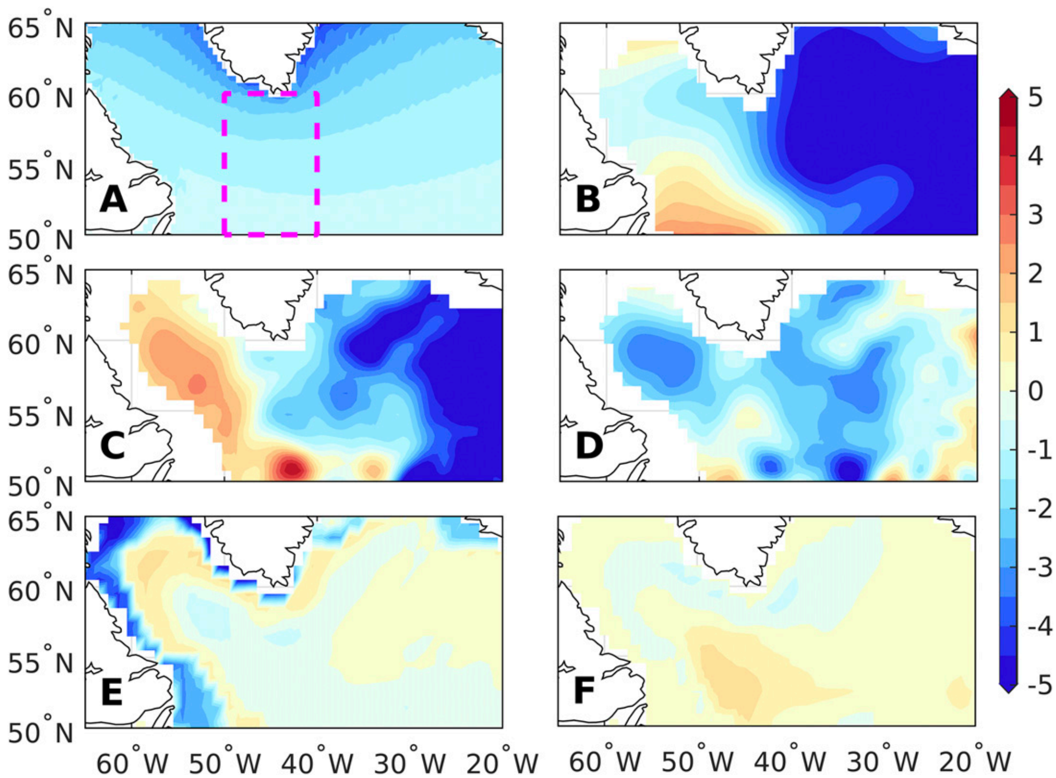


FIG. 2. Estimated trends for the period 2005–15 from (a) combined GAL effects of land and atmosphere, (b) $\zeta$ as measured by altimetry, and (c) upper-ocean steric height as observed by Argo. Spatial mean of $\zeta_L + \zeta_A$ was removed from estimates in (a) and (b). (d) Residual trend of altimetry minus steric height. Similar trends for (e) ocean bottom pressure in equivalent water thickness and (f) steric height below 2000 m, calculated from the ECCO estimate, as described in the text. Units are mm yr$^{-1}$.

the redistribution of water from land to ocean would lead to spatially uniform changes in $\zeta$. The physics of GAL causes deviations from a uniform pattern, with the largest anomalies expected near the regions experiencing significant changes in water storage (Spada and Galassi 2016; Leuliette and Nerem 2016). To highlight GAL impacts, we thus analyze the deviations from the global spatial mean, denoted by the primed variables below. Estimated trends for $\zeta'_L$ (Fig. 1a) are $\pm 1$ mm yr$^{-1}$ over most of the ocean, but they reach more than $-2$ mm yr$^{-1}$ near Greenland and west of the Antarctic Peninsula, indicating the importance of the changing ice sheets (Spada and Galassi 2016; Leuliette and Nerem 2016). In fact, excluding mass changes from Greenland and Antarctica leads to considerably smaller and spatially smoother trend patters (Fig. 1b). The GAL effects from atmospheric mass redistribution (not shown) are an order of magnitude weaker than those in Fig. 1a and play a negligible role, at least for the trends of interest here.

Aside from having the largest (negative) $\zeta'_L$ trends, the strongest spatial gradients are also apparent near the ice sheets and adjacent basins. For example, in the Bellingshausen Basin, west of the Antarctic Peninsula, the difference in trends near the coast and at latitudes around the Drake Passage of $\sim$2 mm yr$^{-1}$ amounts to a difference in $\zeta$ of $\sim$2 cm developing across the Southern Ocean over the analysis period. Similar inferences can be made for the subpolar North Atlantic with decadal differences of $\sim$2 cm in $\zeta'_L$ possible across the Labrador Sea. Such surface signals, if assumed to represent depth-independent pressure gradients, can imply substantial but spurious changes in geostrophic transports.[1]

As an example, Fig. 1c shows the decadal change in zonal geostrophic transport per degree latitude implied by the $\zeta'_L$ trends in Fig. 1a. The largest transports, with magnitudes greater than 0.5 Sv per degree latitude (1 Sv $\equiv 10^6$ m$^3$ s$^{-1}$), are found in the areas already noted near the ice sheets and also in the tropics (e.g., Arabian Sea), where $f$ is smaller.

[1] For a given difference $\delta\zeta$, the volume transport under geostrophy is given by $gHf^{-1}\delta\zeta$, where $g$ is the acceleration of gravity, $H$ is the ocean depth, and $f$ is the Coriolis parameter.

Such changes in transports are very large scale, as expected from the spatial patterns in Fig. 1a, and can thus imply substantial accumulated errors—approximately 5 Sv for the latitudinal sections across the Southern Ocean, subpolar North Atlantic, and the Arabian Sea drawn in Fig. 1c. These values are comparable, for example, to estimates of decadal variability in the Southern Ocean (e.g., Hogg et al. 2015) and the subpolar North Atlantic (e.g., Häkkinen and Rhines 2004) derived from altimeter data uncorrected for GAL effects. Thus, $\zeta'_L$ trends are sizable and likely to corrupt any dynamical inferences made based on altimetry and hydrography measurements, if GAL effects are not properly corrected for.

Given its lower latitudes and better coverage from both altimetry and the Argo system, for the remainder of this work we assess in more detail the GAL effects in the subpolar North Atlantic (Fig. 2a). In particular, we are interested in examining how magnitudes of GAL trends compare to $\zeta$ trends corrected for steric effects. The observed altimeter trends in $\zeta$ (Fig. 2b) are dominated by an east–west dipole pattern that seems to be partly related to steric height changes, as estimated from Argo hydrography over the upper 2000 m (Fig. 2c). In the Labrador Sea and the region between Greenland and the Grand Banks, trends in both $\zeta$ and measured steric height are somewhat weaker, and both positive and negative values are seen. Subtracting the steric effects from $\zeta$ removes some of that pattern and leaves more homogeneous trends on the order of 2 mm yr$^{-1}$ (Fig. 2d). These residual trends, even in the presence of considerable noise, apparent in the steric term (Fig. 2c), have magnitudes comparable to the trends in $\zeta'_L + \zeta'_A$ (Fig. 2a), pointing to the importance of accounting for GAL trends when analyzing the observations (note that we are not concerned here with how well the patterns in Figs. 2a and 2d match, only with the relative size of their trends).

To reduce noise in the observations, we examine time series of the various terms averaged over a 10° × 10° region south of Greenland (Fig. 3). Aside from the month-to-month variability present in all series, the time series of $\zeta'_L + \zeta'_A$ is dominated by a long-term trend of $-1.27 \pm 0.09$ mm yr$^{-1}$, where the quoted uncertainty is twice the standard error of the least squares fit assuming white noise residuals. Upper-ocean steric height has relatively large variability but no apparent trend. The altimeter minus steric height residual still has considerable variability at interannual and shorter time scales, but yields a significant trend of $-1.25 \pm 0.88$ mm yr$^{-1}$, of the same sign and magnitude as the $\zeta'_L + \zeta'_A$ estimate. Taken at face value, these results point to the importance of accounting for GAL effects when interpreting the altimeter

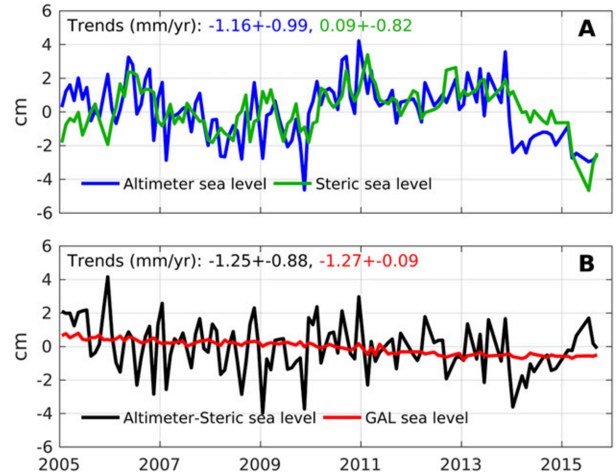


FIG. 3. Time series for average fields over the 10° × 10° region south of Greenland shown in Fig. 2a: (a) Argo steric height (green) and altimetric $\zeta$ minus spatial mean of $\zeta_L + \zeta_A$ (blue), and (b) residual of altimetric minus steric height series (black) and $\zeta'_L + \zeta'_A$ (red). Trends for each curve and their respective uncertainties (twice the standard error) are provided in each panel. Time series of the spatial mean of $\zeta_L + \zeta_A$ (not shown) has a trend of $2.03 \pm 0.1$ mm yr$^{-1}$. Annual cycles have been removed from all time series.

and steric height trends. One would run the risk of seriously confounding $\zeta$ budgets in this region by missing a term as large as the $\zeta$ trend itself.

Although a closed budget for $\zeta$ trends in the region considered in Fig. 3 is beyond our scope, we note that there are two terms missing from the analysis so far: steric changes over depths below 2000 m not sampled by Argo and bottom pressure variability associated with ocean dynamics. Determining deep steric height trends from available data is difficult, but existing basinwide estimates are much smaller than 1 mm yr$^{-1}$ (Purkey and Johnson 2010; Sutton and Roemmich 2011; Desbruyères et al. 2016) with possibly larger values in particular regions (Volkov et al. 2017). Bottom pressure trends derived from GRACE would of course include both dynamic and static effects, but more importantly they are also affected by strong leakage of land signals and thus are not useful over the region of interest. As an alternative, Figs. 2e and 2f show estimates of bottom pressure (in water thickness equivalent) and deep steric trends, respectively, based on the ECCO solution described in Fukumori et al. (2017). The estimates suggest that in this region and for 2005–15 these effects have typical magnitudes of ~1 mm yr$^{-1}$ and can be cancelling at places. Thus, in a general context, GAL effects are as large—if not larger—than other missing terms in the $\zeta$ trend budget and are certainly an important factor to consider in any such analyses.

## 4. Concluding remarks

The importance of correcting altimetric estimates of $\zeta$ for vertical crustal motions has been recognized, first in terms of GIA (Peltier 2001; Huang et al. 2013) and more recently for present-day loading processes (Ray et al. 2013). We argue that when considering the full effects of GAL, as done here, the need for a correction of $\zeta$ records is just as compelling. Such estimates can be based on GRACE data as done here, or a combination of other data and models, particularly for the pre-GRACE period.

Removing such corrections from altimeter measurements of $\zeta$ seems already important when assessing long-term trends in $\zeta$ in terms of surface pressure gradients and geostrophic transports, and this will become only more crucial as records are extended in the future and the effects of land ice become relatively larger, compared to other dynamical trends in $\zeta$. Similar GAL corrections will also be essential for the proper dynamical interpretation of bottom pressure records, when sufficiently accurate estimates become available.

*Acknowledgments.* The NASA GRACE Science Team (Grant NNH16CT00C) and the Sea Level Change Team (Grants NNX14AJ51G and NNX14AP33G) supported this work. We thank C. Little and two anonymous reviewers for their helpful comments on the manuscript. GRACE land data are available online (http://grace.jpl.nasa.gov, which is supported by the NASA MEaSUREs Program).

REFERENCES

Adhikari, S., and E. R. Ivins, 2016: Climate-driven polar motion: 2003–2015. *Sci. Adv.*, **2**, e1501693, https://doi.org/10.1126/sciadv.1501693.

Chelton, D. B., J. C. Ries, B. J. Haines, L.-L. Fu, and P. S. Callahan, 2001: Satellite altimetry. *Satellite Altimetry and Earth Sciences: A Handbook of Techniques and Applications*, L.-L. Fu and A. Cazenave, Eds., International Geophysics Series, Vol. 69, Academic Press, 1–131, https://doi.org/10.1016/S0074-6142(01)80146-7.

Conrad, C. P., and B. H. Hager, 1997: Spatial variations in the rate of sea level rise caused by the present-day melting of glaciers and ice sheets. *Geophys. Res. Lett.*, **24**, 1503–1506, https://doi.org/10.1029/97GL01338.

Desbruyères, D. G., S. G. Purkey, E. L. McDonagh, G. C. Johnson, and B. A. King, 2016: Deep and abyssal ocean warming from 35 years of repeat hydrography. *Geophys. Res. Lett.*, **43**, 10 356–10 365, https://doi.org/10.1002/2016GL070413.

Dobslaw, H., F. Flechtner, I. Bergmann-Wolf, C. Dahle, R. Dill, S. Esselborn, I. Sasgen, and M. Thomas, 2013: Simulating high-frequency atmosphere-ocean mass variability for dealiasing of satellite gravity observations: AOD1B RL05. *J. Geophys. Res. Oceans*, **118**, 3704–3711, https://doi.org/10.1002/jgrc.20271.

Farrell, W. E., and J. A. Clark, 1976: On postglacial sea level. *Geophys. J. Int.*, **46**, 647–667, https://doi.org/10.1111/j.1365-246X.1976.tb01252.x.

Flechtner, F., H. Dobslaw, and E. Fagiolini, 2015: AOD1B product description document for product release 05 (Rev. 4.3). GeoForschungsZentrum Potsdam GRACE Doc. 327-750 (GR-GRZ-AOD-0001), 34 pp., https://www.gfz-potsdam.de/fileadmin/gfz/sec12/pdf/GRACE/AOD1B/AOD1B_20150423.pdf.

Forget, G., J.-M. Campin, P. Heimbach, C. N. Hill, R. M. Ponte, and C. Wunsch, 2015: ECCO version 4: An integrated framework for non-linear inverse modeling and global ocean state estimation. *Geosci. Model Dev.*, **8**, 3071–3104, https://doi.org/10.5194/gmd-8-3071-2015.

Fukumori, I., O. Wang, I. Fenty, G. Forget, P. Heimbach, and R. M. Ponte, 2017: ECCO version 4 release 3. California Institute of Technology Jet Propulsion Laboratory Tech. Rep., 10 pp., ftp://ecco.jpl.nasa.gov/Version4/Release3/.

Gill, A., and P. Niiler, 1973: The theory of the seasonal variability in the ocean. *Deep-Sea Res. Oceanogr. Abstr.*, **20**, 141–177, https://doi.org/10.1016/0011-7471(73)90049-1.

Häkkinen, S., and P. B. Rhines, 2004: Decline of subpolar North Atlantic circulation during the 1990s. *Science*, **304**, 555–559, https://doi.org/10.1126/science.1094917.

Hogg, A. M., M. P. Meredith, D. P. Chambers, E. P. Abrahamsen, C. W. Hughes, and A. K. Morrison, 2015: Recent trends in the Southern Ocean eddy field. *J. Geophys. Res. Oceans*, **120**, 257–267, https://doi.org/10.1002/2014JC010470.

Huang, Z., J.-Y. Guo, C. K. Shum, J. Wan, J. Duan, H. S. Fok, and C.-Y. Kuo, 2013: On the accuracy of glacial isostatic adjustment models for geodetic observations to estimate Arctic Ocean sea-level change. *Terr. Atmos. Oceanic Sci.*, **24**, 471–490, https://doi.org/10.3319/TAO.2012.08.28.01(TibXS).

Jensen, L., R. Rietbroek, and J. Kusche, 2013: Land water contribution to sea level from GRACE and Jason-1 measurements. *J. Geophys. Res. Oceans*, **118**, 212–226, https://doi.org/10.1002/jgrc.20058.

Kendall, R. A., J. X. Mitrovica, and G. A. Milne, 2005: On post-glacial sea level—II. Numerical formulation and comparative results on spherically symmetric models. *Geophys. J. Int.*, **161**, 679–706, https://doi.org/10.1111/j.1365-246X.2005.02553.x.

Kopp, R. E., J. X. Mitrovica, S. M. Griffies, J. Yin, C. C. Hay, and R. J. Stouffer, 2010: The impact of Greenland melt on local sea levels: A partially coupled analysis of dynamic and static equilibrium effects in idealized water-hosing experiments. *Climatic Change*, **103**, 619–625, https://doi.org/10.1007/s10584-010-9935-1.

Le Traon, P.-Y., and R. Morrow, 2001: Ocean currents and eddies. *Satellite Altimetry and Earth Sciences: A Handbook of Techniques and Applications*, L.-L. Fu and A. Cazenave, Eds., International Geophysics Series, Vol. 69, Academic Press, 171–215, https://doi.org/10.1016/S0074-6142(01)80148-0.

Leuliette, E. W., and R. S. Nerem, 2016: Contributions of Greenland and Antarctica to global and regional sea level change. *Oceanography*, **29** (4), 154–159, https://doi.org/10.5670/oceanog.2016.107.

Mitrovica, J. X., and W. Peltier, 1991: On postglacial geoid subsidence over the equatorial oceans. *J. Geophys. Res.*, **96**, 20 053–20 071, https://doi.org/10.1029/91JB01284.

——, M. Tamisiea, J. Davis, and G. Milne, 2001: Recent mass balance of polar ice sheets inferred from patterns of global sea-level change. *Nature*, **409**, 1026–1029, https://doi.org/10.1038/35059054.

Peltier, W. R., 2001: Global glacial isostatic adjustment and modern instrumental records of relative sea level history. *Sea Level Rise: History and Consequences*, B. C. Douglas, J. S. Kearney, and S. P. Leatherman, Eds., International Geophysics Series, Vol. 75, Academic Press, 65–95, https://doi.org/10.1016/S0074-6142(01)80007-3.

Ponte, R. M., and S. V. Vinogradov, 2007: Effects of stratification on the large-scale ocean response to barometric pressure. *J. Phys. Oceanogr.*, **37**, 245–258, https://doi.org/10.1175/JPO3010.1.

Purkey, S. G., and G. C. Johnson, 2010: Warming of global abyssal and deep Southern Ocean waters between the 1990s and 2000s: Contributions to global heat and sea level rise budgets. *J. Climate*, **23**, 6336–6351, https://doi.org/10.1175/2010JCLI3682.1.

Ray, R. D., S. B. Luthcke, and T. van Dam, 2013: Monthly crustal loading corrections for satellite altimetry. *J. Atmos. Oceanic Technol.*, **30**, 999–1005, https://doi.org/10.1175/JTECH-D-12-00152.1.

Rietbroek, R., S.-E. Brunnabend, J. Kusche, and J. Schröter, 2012: Resolving sea level contributions by identifying fingerprints in time-variable gravity and altimetry. *J. Geodyn.*, **59–60**, 72–81, https://doi.org/10.1016/j.jog.2011.06.007.

Roemmich, D., and J. Gilson, 2009: The 2004–2008 mean and annual cycle of temperature, salinity, and steric height in the global ocean from the Argo Program. *Prog. Oceanogr.*, **82**, 81–100, https://doi.org/10.1016/j.pocean.2009.03.004.

Spada, G., and G. Galassi, 2016: Spectral analysis of sea level during the altimetry era, and evidence for GIA and glacial melting fingerprints. *Global Planet. Change*, **143**, 34–49, https://doi.org/10.1016/j.gloplacha.2016.05.006.

Sutton, P., and D. Roemmich, 2011: Decadal steric and sea surface height changes in the Southern Hemisphere. *Geophys. Res. Lett.*, **38**, L08604, https://doi.org/10.1029/2011GL046802.

Tamisiea, M. E., E. M. Hill, R. M. Ponte, J. L. Davis, I. Velicogna, and N. T. Vinogradova, 2010: Impact of self-attraction and loading on the annual cycle in sea level. *J. Geophys. Res.*, **115**, C0700, https://doi.org/10.1029/2009JC005687.

Vinogradova, N. T., R. M. Ponte, M. Tamisiea, J. Davis, and E. Hill, 2010: Effects of self-attraction and loading on annual variations of ocean bottom pressure. *J. Geophys. Res.*, **115**, C06025, https://doi.org/10.1029/2009JC005783.

——, ——, K. J. Quinn, M. E. Tamisiea, J.-M. Campin, and J. L. Davis, 2015: Dynamic adjustment of the ocean circulation to self-attraction and loading effects. *J. Phys. Oceanogr.*, **45**, 678–689, https://doi.org/10.1175/JPO-D-14-0150.1.

Volkov, D. L., S.-K. Lee, F. W. Landerer, and R. Lumpkin, 2017: Decade-long deep-ocean warming detected in the subtropical South Pacific. *Geophys. Res. Lett.*, **44**, 927–936, https://doi.org/10.1002/2016GL071661.

Watkins, M. M., D. N. Wiese, D.-N. Yuan, C. Boening, and F. W. Landerer, 2015: Improved methods for observing Earth's time variable mass distribution with GRACE using spherical cap mascons. *J. Geophys. Res. Solid Earth*, **120**, 2648–2671, https://doi.org/10.1002/2014JB011547.

Watson, C. S., N. J. White, J. A. Church, M. A. King, R. J. Burgette, and B. Legresy, 2015: Unabated global mean sea-level rise over the satellite altimeter era. *Nat. Climate Change*, **5**, 565–568, https://doi.org/10.1038/nclimate2635.